Euronoise 2015 Maastricht

On the use of ship radiated noise to determine statistical information on geoacoustic structure in shallow water from maximum entropy approach

D. P. Knobles
Applied Research Laboratories, University of Texas at Austin, Austin, Texas, USA.

Summary
The use of ambient noise as a means of inferring physical properties of the ocean is of significant interest in ocean acoustics. This study employs the received acoustic field generated by the passage of the R/V Knorr on the New Jersey continental shelf to estimate probability distributions for both the aspect dependent source levels and parameters that represent the geoacoustic structure of the seabed. The statistics of the error function, needed to uniquely specify the likelihood function, are estimated with a maximum entropy approach by creating a data ensemble that includes samples from time periods where the ship-receiver geometry is dominated by either the stern or bow aspect. This method has its origins from the observation that Bayes rule is symmetric with the interchange of the data space and the hypothesis space. The ambiguity between the source levels and the environmental parameters motivate an attempt to *decouple* these parameters through the use of short- and long-range data of the received acoustic field.

PACS no. 43.30.Ma, 43.40.Nb

1. Introduction

This manuscript focuses on the use of ship radiated noise at N frequencies (f_i, $i = 1, 2, ..., N-1, N$) to infer statistical information on the geoacoustic properties of a seabed characterized by a high speed sand layer in a shallow water ocean environment. The linear response problem is defined as

$$P_i = G_i \chi_i \quad , \tag{1}$$

where P_i, χ_i, G_i are the measured pressure field in the water column, the source strengths, and Green's function solution to the wave equation, respectively. G_i depends on the bottom boundary conditions which in turn depend on the geoacoustic structure of the seabed. A complicating feature of G_i is that f_i enters not only directly in the phase of the propagator, but also indirectly via the frequency dependence of the sound speed and attenuation of the medium.

Of special interest for a sand bottom is the sound speed ratio R at the water-sediment interface and the compressional attenuation of the first sediment layer. While the sound speed in the sediment is well approximated to be frequency independent below 1 kHz, this is not the case for the attenuation. The sediment attenuation $A(f)$ in units of dB/m for a single homogeneous sediment layer can, over a small enough frequency band, be expressed as

$$A(f) = \alpha(f/1000)^{\gamma} \quad , \tag{2}$$

where α and f have units of dB/m at 1 kHz and Hz, respectively, and γ is referred to as the frequency exponent. Because of the *mode stripping* effect, information on R, α, and γ is important for the prediction of the statistics of long-range broadband transmission loss. For sand sediments, γ has been reported to be about 1.8 for $f < 1$ kHz [1].

A difficulty of using ship radiated noise to infer the statistics parameters for G_i, such as the seabed geoacoustic parameters, is that the χ_i are generally unknown and aspect dependent. Since Eq. 1 shows a clear ambiguity between source strength and loss parameters in G_i such as the attenuation, it is clear that χ_i must be part of the statistical inference problem. Tollefson and Dosso were the first to apply a Bayesian inference approach, rather than a geoacoustic inversion method, using ship radiated noise to obtain information about both the geoacoustic properties of the seabed and χ_i for selected frequencies[2]. It was assumed that γ was equal to unity. In the current work marginal probability distributions for R, α, γ, and source level $SL_i = 20\log_{10}(|\chi_i|)$ are computed with a maximum entropy (ME) statistical inference methodology from the radiated broadband noise in the 60-695 Hz band emitted by a research vessel recorded on the New Jersey continental shelf in 2006.

2. Acoustic measurements

During 08:00-11:00 Coordinated Universal Time on September 06, 2006, as part of a seabed acoustics experiment on the New Jersey continental shelf [3], the R/V Knorr traveled along an approximate straight line path with a closest point of approach (CPA) of about 1.1 km to a bottom-mounted horizontal line array (HLA). The array was positioned at about 39.2 deg N, 72.97 deg W in about 73 m of water. The uncertainty of the absolute position of the array was about 100 m. From GPS measurements the course of the RV Knorr was determined to be about 213.40 degrees E of N. The speeds of the R/V Knorr over the pre- and post-CPA portions of the track were about 6.71 and 6.68 m/s, respectively. The approximate depth of the propeller of the R/V Knorr is about 2.5 m.

Figure 1 shows a spectrogram recorded on the sixth hydrophone of the HLA. A broadband signature persists for about 25 min on either side of the CPA time, which occurs at approximately Minute of Day (MOD) 562.8. The interfering signals around the 200 and 400 Hz band are caused by moored sources that transmit for 7 min each hour.

In the 50-360 Hz band a *striation* pattern is evident along with high intensity lines superimposed onto the broadband spectrum. The multimode interference pattern responsible for the striations is sensitive to the water column sound speed profile, the water depth, the CPA range (R_{CPA}), the speed of the ship, and the sound speed structure of the seabed, but does not depend in a significant manner on α and γ. Of course, if the loss due to attenuation is too high the interference pattern is diminished.

For increasing times relative to CPA and for increasing frequencies, the striation pattern becomes increasingly complicated. One may ascribe this behavior to the increasing number of modes with frequency. The ability to model the details of this portion of the spectrum is difficult as a result of unknown range-dependent inhomogeneities in the water column and the seabed which result in model error. Thus, one can expect that, with increasing frequency and range, less information is available about the sound speed structure of the seabed. However, the nature of the decrease in the received acoustic levels with range and frequency should contain important information about the mode stripping effect, hence information on α and γ. Factors that limit the amount of information that can be obtained from the decrease in levels over long range scales and higher frequencies are signal to noise ratio (SNR), model error, the ambiguities between loss mechanisms in the seabed and source levels, and the ambiguities among α, γ, and R.

3. Approach

3.1. Maximum entropy

Bayes' rule for conditional probabilities is

$$\mathcal{P}(\mathbf{H}|\mathbf{D}) = \mathcal{P}(\mathbf{H})\frac{P(\mathbf{D}|\mathbf{H})}{P(\mathbf{D})} \quad , \tag{3}$$

where $\mathcal{P}(\mathbf{H}|\mathbf{D})$ is the conditional probability that a hypothesis $\mathbf{H}$ is true given the evidence $\mathbf{D}$ and $\mathcal{P}(\mathbf{D}|\mathbf{H})$ is the conditional probability that $\mathbf{D}$ was measured given $\mathbf{H}$ is true. Henceforth we will refer to the evidence $\mathbf{D}$ as the measured data. $\mathcal{P}(\mathbf{H})$ is the prior distribution that is assumed to be true before the data $\mathbf{D}$ became available. It is common to express $\mathcal{P}(\mathbf{D})$ as a normalization

$$\mathcal{P}(\mathbf{D}) = \int \mathbf{dH}\mathcal{P}(\mathbf{D}|\mathbf{H})\mathcal{P}(\mathbf{H})\mathbf{dH}. \tag{4}$$

It is important to note the symmetry in Bayes' rule in the interchange of $\mathbf{D}$ and $\mathbf{H}$. This symmetry was noted by Bilbro and Van den Bout[4] and used to uniquely specify $\mathcal{P}(\mathbf{H}|\mathbf{D})$ in Ref. [5].

The Kullback relative entropy functional [6]

$$\mathcal{S} = -\int d\mathbf{H}\ \mathcal{P}(\mathbf{H}|\mathbf{D}) \ln\frac{\mathcal{P}(\mathbf{H}|\mathbf{D})}{\mathcal{P}(\mathbf{H})} \quad . \tag{5}$$

is used to develop the ME approach. An unbiased estimate of $\mathcal{P}(\mathbf{H}|\mathbf{D})$ is one that maximizes $\mathcal{S}$ subject to the constraints

$$\int d\mathbf{H}\ \mathcal{P}(\mathbf{H}|\mathbf{D}) = 1 \tag{6}$$

and

$$\langle\mathcal{E}\rangle = \int d\mathbf{H}\ \ \mathcal{P}(\mathbf{H}|\mathbf{D})\,\mathcal{E}\,(\mathbf{H},\mathbf{D})\ , \tag{7}$$

where $\langle\mathcal{E}\rangle$ is a specified value for the expectation of $\mathcal{E}$. The resulting conditional PPD, also referred to as a canonical distribution in statistical physics, is

$$\mathcal{P}(\mathbf{H}|\mathbf{D}) = \mathcal{P}(\mathbf{H})\frac{\exp\left[-\beta\,\mathcal{E}\,(\mathbf{H},\mathbf{D})\right]}{Z(\beta)} \quad , \tag{8}$$

where

$$Z(\beta) = \int d\mathbf{H}\ \ \mathcal{P}(\mathbf{H})\exp\left[-\beta\,\mathcal{E}(\mathbf{H},\mathbf{D})\right] \ . \tag{9}$$

$\mathbf{H}$ contains both SL_i and environmental parameters. $\mathcal{E}$ and β_k are the error function and sensitivity factor,

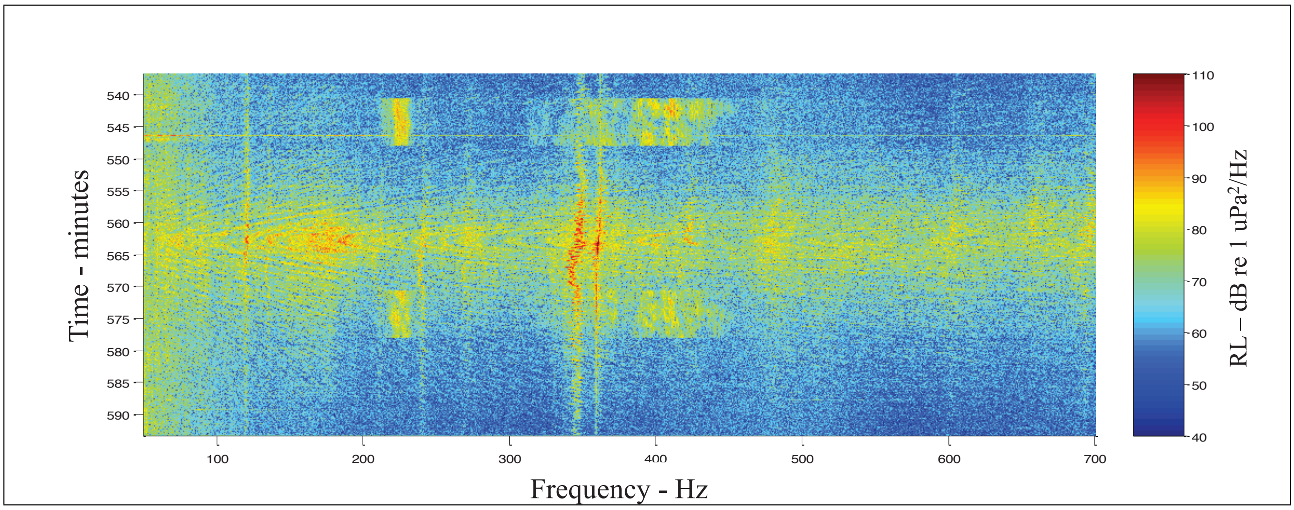

Figure 1. Spectrogram of passage of RV KNORR.

respectively. The error function chosen for this analysis, referred to as the dB error function developed by Koch [7], sums the error of the model and data cross spectra on the array, which eliminates the phase of the source as an unknown, leaving only the magnitude of the source for each frequency. An inherent assumption is that the SL_i are constant over the time segments over which the error function is summed or integrated. $Z(\beta)$ is known as the partition function and acts as a normalization. Equations 8 and 9 are nothing more than Bayes' rule as stated in Eq. (3). The uniqueness of the PPD relies on the determination of the constraint value. Once the unique PPD is determined, the marginal distributions for specific components of $\mathbf{H}$ are obtained by numerical quadrature.

A major focus of Ref. [5] was how to determine β. The same methodology is employed here; namely, the constraint is estimated as

$$\langle \mathcal{E} \rangle_k = \frac{1}{K} \sum_{j=1}^{K} \mathcal{E}([\hat{\mathbf{H}}(\mathbf{D}_k), \mathbf{D}_j) \quad , \tag{10}$$

where the solution that produces the minimum $\mathcal{E}$ is denoted $\hat{\mathbf{H}}$. The k index refers to independent data samples and orginates from the observation of the symmetry of Bayes' rule as discussed by Bilbro [4]. Substituting the canonical distribution and the partition function into the constraint (Eq. 7) allows one to solve for the value of β for each data sample given the value of $\langle \mathcal{E} \rangle_k$. The construction of constraints for this application is nontrivial because one is considering a single passage of a ship. The approach adopted here is to divide the track into two sub tracks where k=1 and k=2 refer to the pre-CPA and post-CPA portion of the source track, respectively. This gives

$$\begin{aligned} \langle \mathcal{E} \rangle_1 = & \frac{1}{2}(\mathcal{E}(\hat{H}((D_1), (D_1)) \\ & + \mathcal{E}(\hat{H}((D_1), (D_2))) \end{aligned} \tag{11}$$

and

$$\begin{aligned} \langle \mathcal{E} \rangle_2 = & \frac{1}{2}(\mathcal{E}(\hat{H}((D_2), (D_2)) \\ & + \mathcal{E}(\hat{H}((D_2), (D_1))) \quad . \end{aligned} \tag{12}$$

A complicating feature of ship-radiated sound is that it generally has an unknown aspect dependence. Thus, for a selection of a range sample that corresponds to a specific range interval, the assumption that the SL_i are constant is likely violated to an unknown degree, and this violation thus becomes part of the average error estimate provided by Eqs. (11-12).

3.2. Prior beliefs and data selection

The first step in the application of ME, or in general a Bayesian approach, to the current problem is to assimilate what one believes to be true prior to the acoustic data becoming available. Of course, if some of these beliefs are not true, this becomes a source of model error in the resulting inferred marginal probability distributions. For the data set being analyzed it is believed that the CPA time, the course of the ship, and the average speed of the ship on either side of CPA are known. Since the course of the ship is 213.4 deg E of N degrees, it is believed that the bearing from the HLA to the ship at CPA time is 303.4 deg E of N. Based on the details of the deployment and ship GPS, it is further believed that the range from the array to the ship at CPA time R_{CPA} is between 1050 and 1200 m.

It is assumed that both the sound speed profile (SSP) in the water column and the geoacoustic representation of the seabed are known, and that both are range-independent. The SSP was derived from two CTD measurements made at 39.201 deg N, 72.965 deg W and at 39.184 deg N, 72.982 deg W, approximately 1.25 and 4.25 hrs after the end of the experiment, respectively. The average of these two measured SSPs is consistent with a warm layer over a

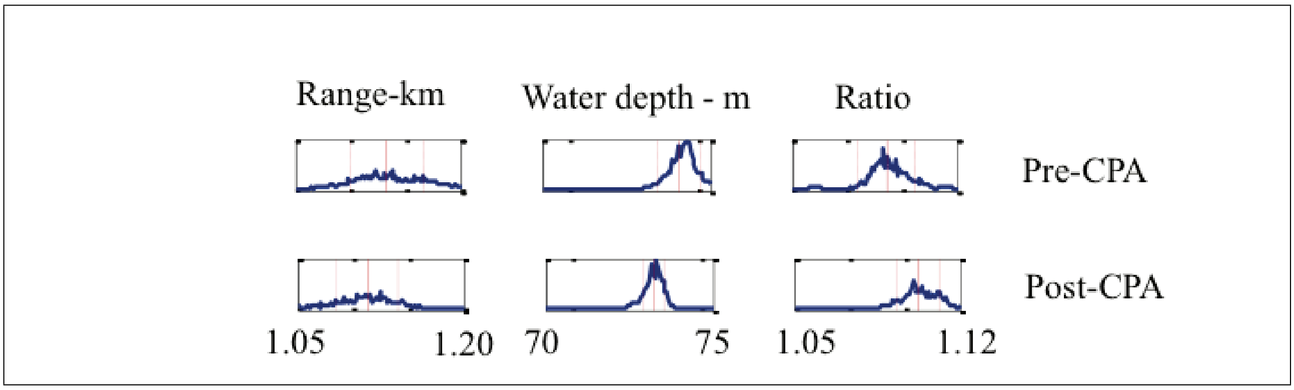

Figure 2. Marginals for R_{CPA}, water depth, and R.

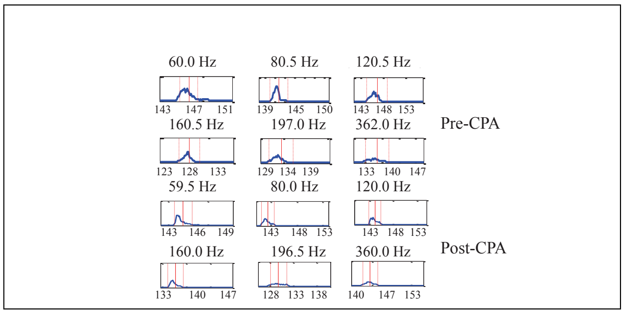

Figure 3. SL_i marginals from short-range data.

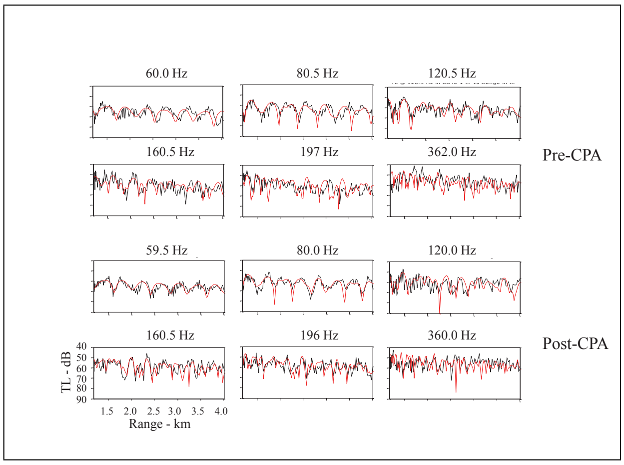

Figure 4. Inversion solutions for TL. Red curves are modeled and black curves are derived from the measured received levels and the inversion solution for the source levels.

colder layer of water. Prior to these measurements on September 01 through September 02, tropical storm Ernesto passed through the area, resulting in an almost *perfect* two-layer water column. It is also believed that on each side of CPA the seabed can be characterized by a range-independent halfspace. The basis of this belief is the existing geophysical information on the seabed in the proximity of the array reported by Santra et al. [8]. The Compressed High Intensity Radar Pulse (CHIRP) database reported in Ref. [8] covers most of the post-CPA portion of the track, but not the pre-CPA portion. The post-CPA track shows a sand layer over what is called the outer-shelf sand layer, where, as the track approaches the array, the top sand layer vanishes, and the outer shelf layer becomes the surface layer. Since the edge of the CHIRP database is very near the array, it is unknown whether or not the outer shelf layer persists or if the surface sand reappears on the pre-CPA track. The grab samples collected by Goff et al. [9] near the array suggests a coarse grained sand with sound speeds in excess of 1700 m/s. As such it is assumed that a half space is a suitable representation for $f > 50$ Hz. It is assumed that the upper and lower bounds for R on each side of CPA are 1.05 and 1.12, respectively, consistent with the acoustical properties of sand. Consistent with the assumption that the SSP and the seabed are range-indepedent along the pre- and post-CPA tracks, it is assumed that the water depth is also range-independent along these tracks with upper and lower bounds 70 and 75 m, respectively.

The next decision is which frequencies to select for the analyses. The selection criteria included the presence of modal interference patterns with four to five maximum and minima on both sides of CPA. This criteria was previously discussed in Ref. [10]. Also, the maximum range was selected such that the SNR was above 6 dB. Also, it was desired to have an approximate symmetry of the received levels with range on either side of CPA. An exact symmetry is not expected because there are Doppler effects, the source is generally aspect dependent, and the ocean environment is not range-independent. The frequencies that were selected for the pre-CPA portion of the track were 60.0, 67.0, 80.5, 89.5, 120.5, 130.5, 135.0, 139.5, 142.5, 146.0, 152.0, 160.5, 162.0, 186.5, 197.0, 250.0, 278.5, 300.50, 362.0, 485.0, 603.0, and 690.0 Hz. The frequencies selected for the post-CPA portion of the track were 59.5,66.0, 80.0, 89, 120.0, 130.5, 135.0, 139.5, 142,5, 146.0, 152.0, 160.5, 162.0, 186.5, 196.0, 250.0, 278.5, 300.50, 360.0, 485.0, 603.0, and 690.0 Hz. Stotts et al. [10] developed a set of criteria along with a numerical implementation in the selection of data.

The above set of frequencies were evaluated with this approach and were found suitable for the inference problem.

4. Results

Monte Carlo integration was generally used to evaluate Eqs. 3, 5, and 6. For all computations, 100,000 samples of **H** were made to compute the conditional PPD. The modeled field computations were made with a range-independent normal mode model [11]. For the computations utilizing the 1-4 km range scale, the sampling of the SL_i was accomplished implicitly as discussed by Dosso[12] without assuming any prior information on the upper and lower bounds. For the computations utilizing the 1-12 km range scale, two types of samplings were made. For the first case the sampling was accomplished implicitly as discussed above; namely, without assuming any prior information on the upper and lower bounds. We will refer to this case as *prior SL statistics not utilized.* In the second case the sampling utilized the SL_i statistics determined from the short-range data. We will refer to this case as *prior SL statistics utilized.* In all computations utilizing the long-range data, in addition to the implicit samplings with upper and lower bounds, random samples in bounded SL space were included. Dosso has referred to this type of sampling as explicit sampling [12].

4.1. Short-range inferences in 60 to 360 Hz band

For the short-range results, the range interval on either side of CPA was about 1.1 to 4.0 km. Figure 2 shows the marginal probability distributions of R_{CPA}, the water depth, and R for pre- and post-CPA range segments. In these computations the frequency band that was utilized was 60-360 Hz where the multimode interference patterns are clearly evident in Fig. 1. The middle red vertical line is the average value and the outer red lines show the standard deviation. The most sensitive parameter, as expected, is the water depth. For both the pre- and post-CPA range intervals, the marginal probability distributions suggest a high sound speed ratio, consistent with the definition of a large-grained sand as reported by Goff et al. [9]. Figure 3 shows SL_i marginal distributions. Overall one observes lower SL_i values for the bow as compared to stern aspect. Also, generally the standard deviation for the SL_i increased with increasing frequency. The standard deviations for the bow aspect SL_i ranged from about 1.35 to 4.5 dB, whereas the standard deviations for the stern aspect SL_i ranged from about 1.10 to 1.85 dB. It is not clear if the increase in the uncertainty of the SL_i for the bow aspect is related to model error associated with the environment or model error associated with the assumption of constant SL_i over a specified range interval. Figure 4 compares the modeled transmission loss for the maximum likelihood or inversion solution to the transmission loss derived from the measured received levels using the inversion solution of the SL_i.

Using the maximum likelihood (inversion) solutions for R_{CPA}, the water depth, and R the SL statistics for 485, 603, and 690 Hz were then established. The reason for this additional step with these higher frequencies relates to the discussion in Sec. 2 that the ability to use higher frequencies to gain information about track parameters and R is degraded due to an increase in model error.

4.2. Long-range inferences

Figure 5 show the marginals for α and γ for the post-CPA long range interval (1.1-12 km). Values for R_{CPA}, R, and the water depth for the pre- and post-CPA computations were held fixed at their maximum likelihood (inversion solution) values from the short-ranged statistical inferences. Four cases are shown. The top left portion of the figure shows the marginal distributions for α and γ in the 60-360 Hz band when the prior statistics on SL_i were not utilized. The top right portion of the figure shows the marginal distributions for α and γ in the 60-360 Hz band when the prior statistics on SL_i were utilized. In both cases the marginal distribution for α shows little structure except to suggest that lower values are less likely than higher values. For γ an average value of 1.75 is observed. The bottom left portion of the figure shows the marginal distributions for α and γ in the 60-690 Hz band when the prior statistics on SL_i were not utilized. The distributions are similar to those observed that utilized the 60-360 Hz band. The bottom right portion of the figure shows the marginal distributions for α and γ in the 60-690 Hz band when the prior statistics on SL_i were utilized. Here one observes that in addition to the marginal distribution for γ having a *peaked* structure, the marginal distribution for α possesses a *peaked* structure with a maximum value of about 0.6 dB/m at 1 kHz.

Thus, it was discovered for the data set considered in this study, that the combination of a large bandwidth (60-690 Hz), large range scales (1-12 km), and the utilization of prior information for SL_i obtained from the shorter range data, it is possible to resolve intrinsic ambiguities and extract meaningful statistical information for both α and γ.

5. CONCLUSIONS

A maximum entropy (ME) approach was employed to compute marginal probability distributions for parameters that characterize the seabed, including the frequency dependence of seabed attenuation using the noise radiated by a large research vessel travelling at

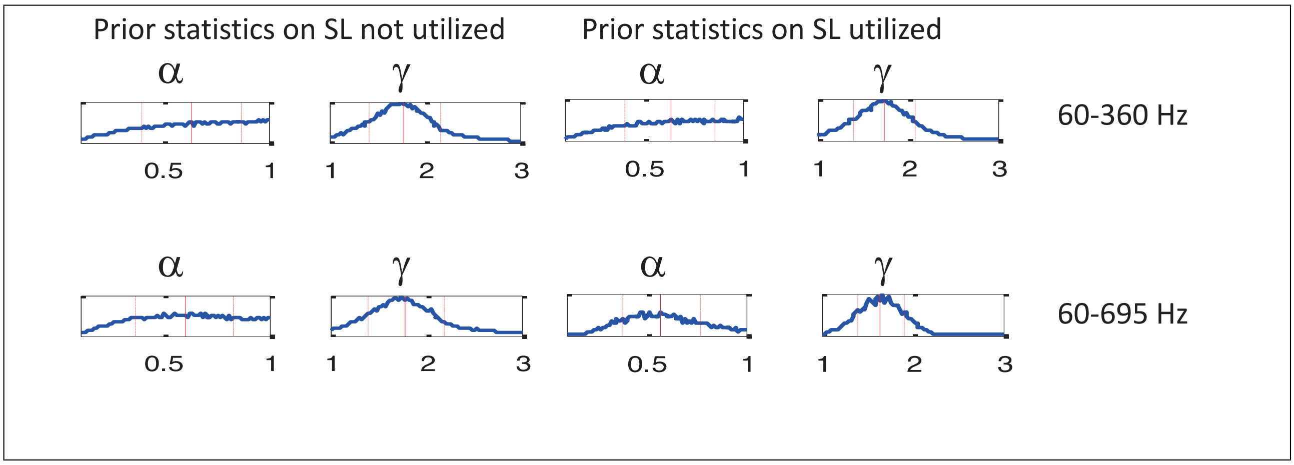

Figure 5. Marginals for α, γ for post-CPA range interval.

about 12 kt. Even though the broadband source levels were much lower than those of a typical merchant ship traveling at a similar speed, the wind noise was low, allowing the radiated noise to be utilized out to ranges of about 150 water depths and frequencies up to about 700 Hz. The method included the concept of first applying a maximum entropy (ME) approach using data with a range scale of about 3 km and a 60 to 360 Hz bandwidth to establish R_{CPA}, the sound speed ratio R at the water-sediment interface, and mean values of the source levels SL_i and their standard deviations. Then, ME was applied again using data with a range scale of about 11 km and a 60 to 690 Hz bandwidth to determine the statistics of the attenuation parameters α and γ. In this second step statistical information about the SL_i obtained in the first step became prior information in the determination of the conditional post probability distribution. In this way the ambiguities between R, SL_i, α, and γ are approximately *resolved*. Measured data acquired on the New Jersey continental shelf were used to test the multisptep ME approach. For range scales of about 11 km and a frequency band of 60 to 690 Hz the average value of α and γ from the marginal distributions of the post-CPA tracks are about 0.60 dB/m at 1 kHz and 1.7, respectively, which are consistent with previous studies for seabeds characterized with sandy sediments[1].

Acknowledgement

This project has been funded by the Office of Naval Research ONR CODE 322 OA.

References

[1] J. X. Zhou, X. Z. Zhang, and D. P. Knobles: Effective geo-acoustic model for sandy seabottoms in shallow water. J. Acoust. Soc. Am. **125**, 2647-2666 (2009).

[2] D. Tollefsen and S. Dosso: Bayesian geoacoustic inversion of ship noise on a horizontal array. J. Acoust. Soc. Am. **124**, 788-795 (2008).

[3] D. P. Knobles, P. S. Wilson, J. A. Goff, and S. E. Cho: A seabed acoustics experiment on a sand ridge on the New Jersey continental shelf. J. Acoust. Soc. Am. **124**, EL151-EL156 (2008).

[4] G. Bilbro and D. E. Van den Bout: Maximum entropy and learning theory. Neural Comp. **4** 839-853 (1992).

[5] D. P. Knobles, J. D. Sagers, and R. A. Koch: Maximum entropy approach to statistical inference for an ocean acoustic waveguide. J. Acoust. Soc. Am. **131**, 1087-1101 (2012).

[6] S. Kullback and R. A. Leibler: On information and sufficiency. The Annals of Mathematical Statistics **22**, 79 86 (1951).

[7] R. A. Koch: Proof of prinicple for inversion of vector sensor array data. J. Acoust. Soc. Am. **128**, 590-599 (2010).

[8] M. Santra, J. A. Goff, J. A. Austin, and R. S. Steel: CHIRP seismic reflection study of falling-stage (forced regressive) sediment wedges on the New Jersey outer continental shelf. Eos Trans. AGU, vol. 88, Fall Meet. Suppl., Abstract OS53A-0983, 2007.

[9] J. A. Goff, B. J. Kraft, L. A. Mayer, S. G. Schock, C. K. Sommerfield, H. C. Olson, S. P. S. Gulick, and S. Nordfjord: CHIRP seismic reflection study of falling-stage (forced regressive) sediment wedges on the New Jersey outer continental shelf. Mar. Geol., **209**, 147-172, (2004).

[10] S. A. Stotts, R. A. Koch, S. M. Joshi, V. T. Nguyen, and D. P. Knobles: Geoacoustic inversions of horizontal and vertical line array acoustic data from a surface ship of opportunity. IEEE J. Oceanic Eng. **35**, 79-102 (2010).

[11] R. A. Koch and J. E. LeMond, Software Requirements Specification for the NAUTILUS Model (Version 1.0), ARL-TL-EV-01-18, April 2001.

[12] Stan E. Dosso and Michael J. Wilmut: Maximum-likelihood and other processors for incoherent and coherent matched-field localization. J. Acoust. Soc. Am. **132**, 2273-2285 (2012).